

On Product Codes with Probabilistic Amplitude Shaping for High-Throughput Fiber-Optic Systems

Alireza Sheikh *Member, IEEE*, Alexandre Graell i Amat, *Senior Member, IEEE*,
and Alex Alvarado, *Senior Member, IEEE*

Abstract—We consider probabilistic amplitude shaping (PAS) as a means of flexibly varying the spectral efficiency of fiber-optic communication systems. Recently, the PAS architecture originally proposed for a coded modulation (CM) scheme with soft decision decoding has been applied to bit-wise hard decision decoding (HDD) of staircase code. In this paper, we apply the PAS to bit-wise HDD based on the product codes (PCs). We show that the PAS with PCs yields significant gains up to approximately 1 bit/channel use with respect to the baseline scheme using PC with uniform signaling. We also show that the performance of PAS with PC is close to that of PAS with staircase codes. Furthermore, we show that by combining our recently proposed soft-assisted decoder for PCs with the PAS architecture, one can achieve even better operating point than that of PAS with staircase codes decoded using conventional bounded distance decoding.

Index Terms—Coded modulation, error correcting codes, hard decision decoding, probabilistic shaping, product codes, optical networks, signal shaping.

I. INTRODUCTION

THE ever increasing data demand for fiber optic communication has been mainly driven by the massive growth of the internet users as well as cloud-based applications. To keep up with the current trend on data demand, utilize higher spectral efficiencies and improve the transmission reach, coding in combination with a high order modulation, a scheme known as coded modulation (CM), has become indispensable in fiber-optic communications. For instance, a recently commercially available optical transponder viable of providing 400 Gbit/s/λ and 600 Gbit/s/λ with maximum reach of 1500 km and 150 km, respectively, employs up to 64 quadrature amplitude modulation (QAM) [1].

In a practical CM scheme, there is always a gap between the performance of the CM system and the corresponding theoretical limit. This gap is mainly due to two reasons. First, the employed codes are of finite length and suboptimal decoders are usually employed in order to constrain the receiver complexity. Second, uniform signaling with equidistant signal constellation points (squared QAM) yields 1.53 dB gap

to the Shannon limit for an additive white Gaussian noise (AWGN) channel in the asymptotically large signal dimension and signal-to-noise ratio (SNR) [2].

In order to enhance the performance of the CM system and operate close to the Shannon limit, one approach is to improve the decoding performance of the employed codes. There are two main types of decoding architectures, namely soft decision decoding (SDD) and hard decision decoding (HDD). SDD provides large net coding gains suitable for long distance transmission at the cost of high decoding data flow, power consumption, and circuit area [3]. This makes the adoption of SDD-based codes such as low density parity check (LDPC) codes [4] and turbo product codes [5] for the next generation high-throughput low-power fiber-optic applications very challenging. On the other hand, HDD entails up to two orders of magnitude lower decoder data flow [6] and power consumption [7] than that of SDD at the cost of some performance loss compared to SDD. Product codes (PCs) [8] and staircase codes [6] with bounded distance decoding (BDD) of the component codes are the major two classes of HDD codes suitable for very high-throughput applicants such as next generation fiber-optic communication. For instance, PCs have been adopted by the optical submarine standard [9] and staircase codes has been considered as an outer code for 400G ZR standard for transmission at 400 Gbps over data center interconnect links up to 100 km [10]. An interesting line of research is to close the gap between HDD and SDD while maintaining the decoding complexity close HDD. This has recently attracted attention in both academia [11]–[18] and industry [19]–[21].

An alternative approach to close the gap between performance of the CM scheme and theoretical limits is to employ signal shaping. The gist of the signal shaping technique is to mimic the capacity achieving distribution by adjusting the position of the constellation points with uniform signaling, known as geometric shaping [22]–[26], and/or adjusting the probability of occurrence for equidistant signal points, known as probabilistic shaping [27]–[29]. A novel family of probabilistic shaping schemes, known as probabilistic amplitude shaping (PAS), was proposed in [29]. PAS has attracted a great deal of interest in the fiber-optic community [30]–[34]. The structure of PAS allows to flexibly change the spectral efficiency without changing the decoder architecture. In particular, it has been shown that PAS with an LDPC code and SDD [29] as well as PAS with staircase codes and HDD [35] achieve a wide range of spectral efficiencies with significant gains compared to the baseline CM with uniform

The work of A. Sheikh and A. Alvarado has received funding from the European Research Council (ERC) under the European Union's Horizon 2020 research and innovation programme (grant agreement No 757791). A. Graell i Amat was supported by the Swedish Research Council under grant 2016-04253.

A. Sheikh and A. Alvarado are with the Department of Electrical Engineering, Eindhoven University of Technology, 5612 AZ Eindhoven, The Netherlands (email: {a.sheikh,a.alvarado}@tue.nl).

A. Graell i Amat is with the Department of Electrical Engineering, Chalmers University of Technology, SE-41296 Gothenburg, Sweden (email: alexandre.graell@chalmers.se).

signaling.

In this paper, we combine the soft-aided decoding algorithm for PCs [11], [12] with the PAS framework to improve the performance of CM with PCs. In particular, similar to [35], we optimize the Maxwell-boltzman type distribution in order to maximize the achievable information rate of PAS with bit-wise HDD. Then we apply the PAS architecture with slight modification to PCs and find the possible transmission modes for a PC with a given Bose-Chaudhuri-Hocquenghem (BCH) component code. Afterwards, we address the selection of the operating points for finite frame length. Finally, we combine a soft-aided decoding algorithm to the presented architecture to improve the performance of the overall system. We show that PAS with PC and BDD of the component codes provides gains up to 2.7 dB gain with respect to the baseline scheme with uniform signaling. Furthermore, we show that an spectral efficiency improvement of up to 1 bit/channel use (bpcu) is given by the proposed scheme. We also show that the soft-aided decoding algorithm improves the operating SNR of the PAS with PC up to 0.295 dB compared to the PAS with PC and standard BDD of the component codes. Interestingly, we show that the combination of the soft-aided decoding algorithm for PCs with the PAS architecture outperforms the PAS with staircase codes and standard BDD of the component codes.

The remainder of the paper is organized as follows. In Section II, the achievable information rate with bit-wise HDD for the PAS scheme is discussed. The CM scheme with PAS and PCs is further elaborated in Sections III and IV. Finally, simulation results are given in Section V and some conclusions are drawn in Section VI.

Notation: The following notation is used throughout the paper. We define the sets $\mathbb{N} \triangleq \{1, 2, \dots\}$ and $\mathbb{N}_0 \triangleq \{0, 1, \dots\}$. We denote by $P_X(\cdot)$ the probability mass function (pmf) and by $p_X(\cdot)$ the probability density function (pdf) of a random variable (RV) X . We use boldface letters to denote vectors and matrices, e.g., \mathbf{x} and \mathbf{X} , respectively. x_i is the i -th element of \mathbf{x} and expectation with respect to the pmf of RV X is denoted by $\mathbb{E}_X(\cdot)$. $H(X)$ stands for entropy of the RV X .

II. ACHIEVABLE INFORMATION RATE WITH HARD DECISION DECODING AND BIT-WISE DECODING

We consider a discrete-time AWGN channel¹ with input-output relation at time instant i

$$Y_i = \Delta X_i + Z_i \quad i = 1, 2, \dots, n, \quad (1)$$

where n is the number of channel uses (i.e., the block length), X_i is the channel input, Y_i is the corresponding output, Δ is a scaling constant, and $\{Z_i\}$ are independent and identically distributed (i.i.d.) Gaussian RVs with zero mean and unit variance. The scaling parameter Δ assures an average transmit power P , i.e.,

$$\mathbb{E}[(\Delta X)^2] = P.$$

According to the definitions above, the SNR is given by $\text{SNR} = P$. We consider a block-wise transmission system

¹The AWGN channel is an accurate model for long-haul coherent fiber-optic communications when the fiber-optic channel is dominated by amplified spontaneous emission noise [36].

where \mathbf{u} denotes the transmitted information block and $\hat{\mathbf{u}}$ denotes the decoded information block. For the sake of simplicity for the analysis and the design of the PAS scheme in the next section, we consider ASK modulation as the underlying modulation. In particular, the channel input alphabet is given by $\mathcal{X} \triangleq \{-2^m + 1, \dots, -1, 1, \dots, 2^m - 1\}$, where m is the number of bits per symbol, and $M = 2^m$ is the number of signal points. We remark that the PAS scheme directly extends to square QAM constellations, as the Cartesian product of two ASK constellations (see also Section IV-B). In Section V we give results for QAM constellations.

Similar to the approach in [35], in this paper we consider the PAS scheme of [29] with a binary code for transmission and bit-wise HDD (i.e., bit-wise Hamming metric decoding) at the receiver side. Denote by $\hat{X} \in \mathcal{X}$ the RV associated with the detector output (hard decision). An achievable rate for the PAS scheme can be computed by resorting to the approach introduced in [37], yielding

$$R_{\text{HDD}} = \sup_{s>0} \left[H(X) + \mathbb{E} \left[\log_2 \frac{q(X, \hat{X})^s}{\sum_{x' \in \mathcal{X}} q(x', \hat{X})^s} \right] \right]^+ \quad (2)$$

where $[a]^+ = \max(0, a)$, s is the optimization parameter, and $q(X, \hat{X})$ is the (mismatched) decoding metric [38], [39]. For HDD, the decoding metric is the bit-wise Hamming metric, which has the equivalent form

$$q(x, \hat{x}) = \varepsilon^{\text{d}_H(\text{L}(x), \text{L}(\hat{x}))}$$

where ε is an arbitrary constant in $(0, 1)$, $\text{L}(x)$ is the m -bit labeling associated with constellation symbol x , and $\text{d}_H(\text{L}(x), \text{L}(\hat{x}))$ is the Hamming distance between the binary labelings of x and \hat{x} . Here, we consider the binary reflected Gray code (BRGC) labeling [40]. Note that the $\mathbb{E}(\cdot)$ function in (2) is over the $P_{\hat{X}|X}(\hat{x}, x)$ where \hat{X} and X are RVs corresponding to transmitted and hard detected symbols, respectively.

Similar to [29], [35], we consider the Maxwell-Boltzmann distribution for the channel input X ,

$$P_X^\lambda(x) = \frac{\exp(-\lambda x^2)}{\sum_{\hat{x} \in \mathcal{X}} \exp(-\lambda \hat{x}^2)}.$$

For each SNR, we select λ such that the achievable rate is maximized, i.e.,

$$\lambda^* = \underset{\lambda}{\text{argmax}} R_{\text{HDD}}. \quad (3)$$

We consider a symbol-wise maximum a-posteriori (MAP) detector that outputs

$$\hat{x} = \underset{x \in \mathcal{X}}{\text{argmax}} p_{Y|X}(y|x) P_X(x) \quad (4)$$

yielding the conditional pmf $P_{\hat{X}|X}$ to be used, jointly with P_X , to compute (2).

In Fig. 1, we compare the achievable rate R_{HDD} of probabilistic shaping and uniform signaling for 4-ASK, 8-ASK, and 16-ASK. As can be seen, there is large gap between the achievable information rate for the shaped constellation

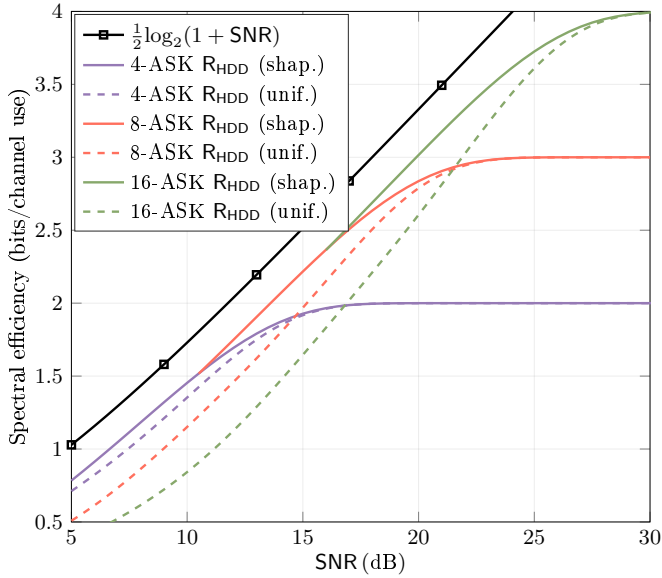


Fig. 1. Comparison between the achievable rates of probabilistic amplitude shaping and uniform signaling with bit-wise HDD.

compared to the uniform one, where the gap increases by the size of the modulation order. Furthermore, by changing the modulation order, the shaped scheme can operate in a roughly constant gap to the capacity of the soft-decision AWGN channel.

III. CODED MODULATION WITH PAS AND PCs

In this section, we apply PAS to HDD and PCs. The CM scheme using PAS is depicted in Fig. 2. The random variable X can be factorized as

$$X = A \cdot S \quad (5)$$

where $A \triangleq |X|$ and $S \triangleq \text{sign}(X)$ are the absolute value (amplitudes) and sign of the RV X , respectively. As observed in [29], $P_X^{\lambda^*}$ is symmetric, i.e., $P_X^{\lambda^*}(x) = P_X^{\lambda^*}(-x)$ for $x \in \mathcal{X}$. Therefore, S is uniformly distributed,

$$P_S(1) = P_S(-1) = \frac{1}{2} \quad (6)$$

while the distribution of A satisfies

$$P_A^{\lambda^*}(a) = 2P_X^{\lambda^*}(a) \quad (7)$$

where $a \in \mathcal{A} \triangleq \{1, \dots, 2^m - 1\}$ with size of 2^{m-1} .

The idea of PAS is to shape the constellation amplitudes and then utilize the parity bits generated by a systematic encoder to represent the sign bits. Therefore, the information sequence \mathbf{u} is split into two sequences \mathbf{u}^s and \mathbf{u}^a . The sequence \mathbf{u}^a is used to generate a sequence of amplitudes a_1, \dots, a_n with the desired distribution. The binary image of the amplitudes and the remaining information bits, i.e., those belonging to \mathbf{u}^s , are then encoded using a systematic binary encoder. The parity bits generated by the systematic encoder and \mathbf{u}^s are used to generate n sign labels s_1, \dots, s_n . Assuming uniform distribution of the information bits and since the parity bits at the output of the encoder tend to be uniformly distributed as well, the sign labels closely mimic the desired (uniform) distribution (6).

A. Amplitude Shaping and Amplitude-to-Bit (ab) Mapping

Let $\mathbf{u} = (u_1, \dots, u_{k+\gamma n})$ be the information sequence of length k bits, $u_i \in \{0, 1\}$. Information bits are modeled as uniformly-distributed i.i.d. RVs. The vector \mathbf{u} is split into two vectors \mathbf{u}^s and \mathbf{u}^a , of lengths γn and k , respectively, where γ is a tuning parameter whose meaning will become clear later and it is assumed that $\gamma n \in \mathbb{N}_0$. Vector \mathbf{u}^a is used to generate a sequence of amplitudes $\mathbf{a} = (a_1, \dots, a_n)$ with distribution $P_A^{\lambda^*}$ through a shaping block. The binary interface which generates the sequence of amplitudes with a given distribution (in our case $P_A^{\lambda^*}$) from a uniformly distributed input is called the *distribution matcher*. The distribution matchers proposed in the literature can be categorized in two groups, variable-length [41]–[44] and fixed-length [45]–[47] distribution matchers. To limit error propagation, we consider fixed-length distribution matching. As will be shown in Sec. III-B, the block length considered in this paper is large (in the order of 12k–260k), hence there is no difference in terms of rate loss between the distribution matchers in [45]–[47]. In this regard, we use the *constant composition distribution matching* (CCDM) method proposed in [45] as the most popular distribution matcher in the literature. We refer the interested reader to [29, Sec. V] and [45] for more details. The rate of the shaping block is k/n and it approaches $H(A)$ for large n .

To reduce the number of bit errors associated with a symbol error, we consider the BRGC labeling. In the mapping part, for an M -ASK modulation with $m = \log_2 M$ bits per symbol, the sequence of amplitudes a_1, \dots, a_n is transformed into a sequence of bits using the mapper Φ_{ab} . We label each of the amplitudes a_i with $m - 1$ bits (size of \mathcal{A} is 2^{m-1}) using the BRGC labeling to construct a binary string $\mathbf{b}_i \triangleq \mathbf{b}(a_i) = (b_1^i, \dots, b_{m-1}^i)$. The sequence $\mathbf{b} = (\mathbf{b}_1, \dots, \mathbf{b}_n)$ is of length $\ell = n(m - 1)$ bits.

B. Encoding

The sequences \mathbf{b} and \mathbf{u}^s are multiplexed and encoded by a binary linear block code with a systematic encoder. As binary linear block codes, we use PCs with Bose-Chaudhuri-Hocquenghem (BCH) codes as component codes. In particular, we consider (n_c, k_c) systematic BCH component codes of code length n_c and dimension k_c . Let \mathcal{C} be an (n_c, k_c) shortened BCH code constructed over the Galois field $\text{GF}(2^v)$ with (even) block length n_c and information block length k_c given by

$$\begin{aligned} n_c &= 2^v - 1 - s, \\ k_c &= 2^v - vt - 1 - s \end{aligned}$$

where s and t are the shortening length and the error correcting capability of the code, respectively. A shortened BCH code is thus completely specified by the parameters (v, t, s) . A PC with (n_c, k_c) component codes is defined as the set of all $n_c \times n_c$ matrices $\mathbf{C} = [c_{i,j}]$ such that each row and column of the matrix \mathbf{C} is a valid codeword of \mathcal{C} . Fig. 3 shows the code array of a PC. The red parts correspond to the information bits while the parity bits are shown with blue hatches.

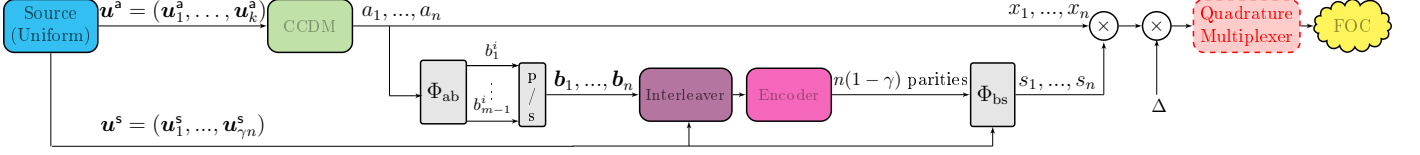


Fig. 2. Block diagram of the CM scheme with PAS and PC under consideration. The parameters shown in the system model corresponds to encoding of one PC code array.

Table I
PARAMETERS OF THE DESIGNED PCs FOR $v = 10$, $t = 3$, AND 16-ASK MODULATION

γ	0.7682	0.7503	0.6912	0.6797	0.5942	0.5233	0.4464	0.3645	0.2303	0.1426	0.0085
s	3	77	261	289	447	535	605	661	727	759	797
n_c	1020	946	762	734	576	488	418	362	296	264	226
k_c	990	916	732	704	546	458	388	332	266	234	196
n	260100	223729	145161	134689	82944	59536	43681	32761	21904	17424	12769
γn	199800	167869	100341	91549	49284	31156	19501	11941	5044	2484	109
R_{PC}	0.9420	0.9376	0.9228	0.9199	0.8985	0.8808	0.8616	0.8411	0.8076	0.7856	0.7521

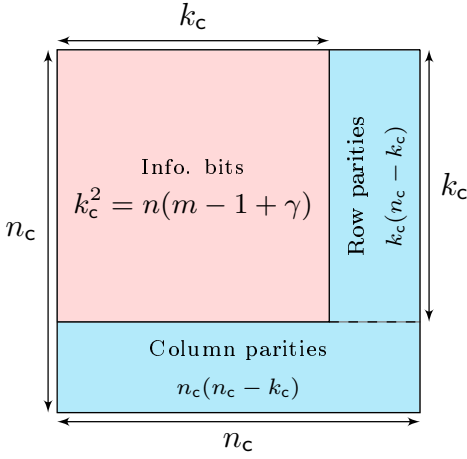


Fig. 3. Code array of a PC. The red colored area shows the information bits while the colored blue area corresponds to the parity bits generated by row and column encoding.

The rate of the PC with (n_c, k_c) BCH component codes is

$$R_{PC} = \frac{k_c^2}{n_c^2}. \quad (8)$$

For a 2^m -ASK constellation, we assume a staircase code with code rate

$$R_{PC} = \frac{k_c^2}{n_c^2} = \frac{m-1+\gamma}{m} \quad (9)$$

where $0 \leq \gamma < 1$ is a tuning parameter which can be used to select the rate of the PC and subsequently the spectral efficiency of the CM scheme. We assume that at time instance i , each shaped amplitude block corresponds to one PC codeword, i.e., C_i .

For (n_c, k_c) component codes, each matrix C_i of the PC array contains k_c information bits per row, i.e., a total of k_c^2 information bits (see Fig. 3). Consequently, we parse the sequences \mathbf{b} and \mathbf{u}^s into blocks of length n and γn , respectively, such that

$$n = \frac{k_c^2}{m-1+\gamma}$$

where the parameters (n_c, k_c) , and hence γ , are chosen such that n and γn are integers. Using (9), it follows that the total number of parity bits corresponding to each array C , $n_c^2 - k_c^2$, is

$$\begin{aligned} n_c^2 - k_c^2 &= n(m-1+\gamma) \left(\frac{1}{R_{PC}} - 1 \right) \\ &= n(m-1+\gamma) \left(\frac{m}{m-1+\gamma} - 1 \right) \\ &= n(1-\gamma). \end{aligned} \quad (10)$$

Lets assume that the bits $\bar{\mathbf{b}}_i \triangleq \mathbf{b}_{i \cdot n+1}, \mathbf{b}_{i \cdot n+2}, \dots, \mathbf{b}_{i \cdot n+n}$ and $\tilde{\mathbf{u}}_i^s \triangleq \mathbf{u}_{i \cdot \gamma n+1}^s, \dots, \mathbf{u}_{i \cdot \gamma n+\gamma n}^s, i = 0, 1, \dots$, are then placed as the information bits in PC code array C_i . In particular, let $\tilde{\mathbf{b}}_i$ the string of bits obtained by randomly interleaving the concatenation of $\bar{\mathbf{b}}_i$ and $\tilde{\mathbf{u}}_i^s$ (see random interleaver in Fig. 3). Then, $\tilde{\mathbf{b}}_i$ is divided into k_c equal parts, $\tilde{\mathbf{b}}_{i,1}, \dots, \tilde{\mathbf{b}}_{i,k_c}$ of lengths $\alpha_b = n(m-1+\gamma)/(k_c)$, and the vector $\mathbf{b}_{i,j}$ is placed in row j of matrix C_i . Note that (n_c, k_c) and γ must be chosen such that

$$n \in \mathbb{N} \quad (11)$$

$$\gamma n \in \mathbb{N}_0. \quad (12)$$

Then, encoding of the PC is performed as usual, by row/column encoding, using the (n_c, k_c) BCH component code (see Fig. 3). We denote by \mathbf{p}_i , the parity bits of matrix C_i of length $n_c^2 - k_c^2$ (shown with blue in Fig. 3) resulting from the encoding process. Note that $k_c(n_c - k_c)$ parities are resulted from encoding of k_c rows of PC and the other $n_c(n_c - k_c)$ parities yields from encoding of n_c columns of C_i .

If the ASK constellation is fixed, to achieve different spectral efficiencies, the code rate of the PC must be changed. For a given modulation order (given m), one can find different feasible solutions for (v, t, s) that lead to a value of γ that satisfies (11), (12), and $n \in \mathbb{N}$.

In Table I some feasible values for s (and therefore γ), the parameters (n_c, k_c) for the resulting BCH component codes, n , and the rate of the PC, R_{PC} , are summarized for 16-ASK modulation ($m = 4$) for $v = 10$ and $t = 3$. The same table for

Table II
BRGC OF THE AMPLITUDES FOR 8-ASK

amplitude	-7	-5	-3	-1	1	3	5	7
label	110	111	101	100	000	001	011	010

staircase codes with 16-ASK modulation ($m = 4$), $v = 10$, and $t = 3$ is given in [35, Table II]. We highlight that the feasible values for s in Table I are only a small subset of a total of 205 feasible values. Furthermore, one can check that the total number of feasible values for s in staircase code is only 40. This means that PAS with PC can essentially provide much finer granularity on the operating point than that of PAS with staircase codes.

C. Bit-to-Sign (bs) Mapping

For each code array block C_i , the parity bits of C_i are multiplexed with \tilde{u}_i^s to generate, through the bit-to-sign mapper Φ_{bs} , the sequence of signs $s = (s_1, \dots, s_n)$, which will be used as the signs of the amplitudes a_1, \dots, a_n . In particular, we combine the block of $n_c^2 - k_c^2$ parity bits with the γn information bits \tilde{u}_i^s to form the vector t_i , of length $n_c^2 - k_c^2 + \gamma n = n$, where we used (10). Then, the binary vector $t_i = (t_1, \dots, t_n)$, of length n bits, is used to form the sequence of n signs s by mapping $s_i = 0$ and $s_i = 1$ to $t_i = +1$ and $t_i = -1$, respectively. As shown in [29], the distribution of the signs closely mimics the uniform one, according to (5)–(7), the element-wise multiplication of (a_1, \dots, a_n) by (s_1, \dots, s_n) generates a sequence $x = (x_1, \dots, x_n)$ with the desired distribution.

Finally, the sequence x is scaled by Δ and transmitted over the fiber-optic channel (FOC).

D. Interleaver

We assume that the sign bits generated by PAS represent the first bit level in the binary label of the transmitted symbol, e.g., the transmuted signal points with the corresponding binary labels for 8-ASK modulation is shown in Table II. From Table II one can readily infer that on average the reliability of first bit level is much larger than other levels, i.e., it is unlikely that the sign of the transmitted symbol is changed due to the Gaussian distribution of the noise. Motivated by the BICM paradigm, we add a random interleaver to the PAS architecture in order to ensure that γn portion of the highly reliable sign bits which are placed as the information bits in the PC array are uniformly distributed between the component codes and hence, the corresponding component codes observe the same average channel. This uniform distribution of highly reliable bits reduces the probability of the stall patterns of size $(t+1)^2$ errors, where the iBDD of PCs can not resolve of such errors. We refer the interested reader to [48, Sec.II] more details about the stall patterns of PCs.

We remark that in the PAS architecture with staircase codes given in [35, Fig. 3], there is no random interleaver, as the design procedure of the staircase code already ensures that the γn sign bits are uniformly distributed between the component codes (see [35, Sec. IV.C]).

E. Decoding

PCs are usually decoded using very low complex iterative bounded-distance decoding (BDD) of the component codes [49]. BDD works as follows. For the decoding of an arbitrary row or column component code, we assume that the codeword $c = (c_1, \dots, c_{n_c})$ taken from the codebook \mathcal{C} is transmitted and the decoding is only based on hard-detected channel observations, i.e., $r = (r_1, \dots, r_{n_c})$. BDD corrects all error patterns with Hamming weight up to the error-correcting capability of the component code, $t = \lfloor \frac{d_{\min}-1}{2} \rfloor$. If the weight of the error pattern is larger than t and there exists another codeword $\tilde{c} \in \mathcal{C}$ with $d_H(\tilde{c}, r) \leq t$, then BDD outputs \tilde{c} and thus introduces a miscorrection. Otherwise, if no such codeword exists, BDD fails and we use the convention that the decoder outputs r . Concisely, the decoded vector \hat{r} for BDD can be written as

$$\hat{r} = \begin{cases} c & \text{if } d_H(c, r) \leq t \\ \tilde{c} \in \mathcal{C} & \text{if } d_H(c, r) > t \text{ and } \exists \tilde{c} \text{ such that } d_H(\tilde{c}, r) \leq t. \\ r & \text{otherwise} \end{cases}$$

The decoding of PCs is usually based on iteratively performing the BDD to row/column codes, which in this paper we referred to as iBDD. Recently, several soft-assisted decoders for PCs has been proposed which provides a clear decoding performance-complexity tradeoff, suitable for high-throughput fiber-optic communications. From a high level view, all these new decoding algorithms modify the core BDD based on the soft information given from the channel in order to improve the performance while keeping the complexity of the decoder close to BDD [11]–[18]. In order to apply these decoding architectures in PAS with PCs, it is required to compute the reliability of the hard detected bits at the decoder. Given the received symbol Y_i (see (1)), one can compute the log-likelihood ratio (LLR) corresponding to l -th ($l \in \{1, \dots, m\}$) bit of the corresponding binary image of X_i as

$$L_i^l = \ln \left(\frac{\sum_{\tilde{X}_i \in S_l^0} e^{-\frac{(Y_i - \Delta \tilde{X}_i)^2}{2}} \cdot P_X^\lambda(\tilde{X}_i)}{\sum_{\tilde{X}_i \in S_l^1} e^{-\frac{(Y_i - \Delta \tilde{X}_i)^2}{2}} \cdot P_X^\lambda(\tilde{X}_i)} \right), \quad (13)$$

where S_l^0 and S_l^1 are sets of size 2^{m-1} ASK symbols with 0 and 1 as the l th bit of the corresponding BRGC label, respectively. In Sec. V the soft-aided decoder of the PCs employs hard detection on the bit level based on (13) and utilizes these reliabilities to modify the outbound messages of the BDD.

IV. DESIGNING THE OPERATING POINTS

A. The Effect of Shaping on the Operating Point

For each PC codeword C_i , the transmitted data is $u_{i \cdot \gamma n + 1}^s, \dots, u_{i \cdot \gamma n + n}^s$ and $u_{i \cdot k + 1}^a, \dots, u_{i \cdot k + k}^a$, which are embedded in the amplitudes $a_{i \cdot n + 1}, a_{i \cdot n + 2}, \dots, a_{i \cdot n + n}$. Therefore, for asymptotically large CCDM output length n , the rate is $R = H(A) + \gamma$ [bits/channel use]. For small values of n , the operating point is $\frac{k}{n} + \gamma$ [bits/channel use]. For the feasible

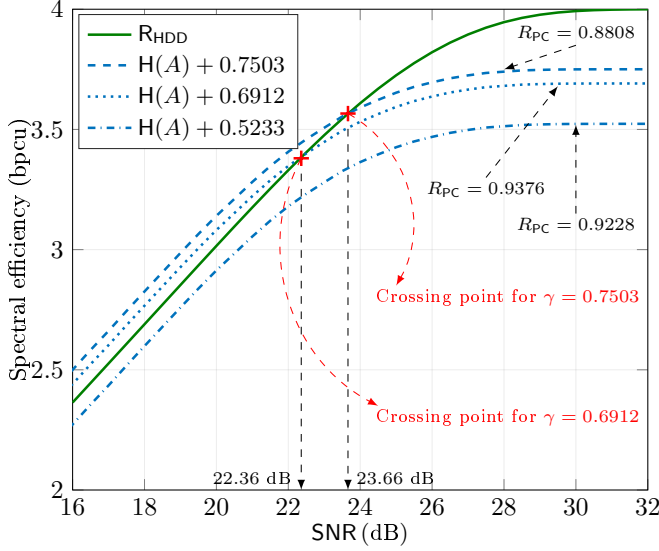


Fig. 4. An example for determining the feasible SNR region depending on the selected γ corresponding to some of the designed codes for 16-ASK.

values of s given in Table I, n is large, i.e., $\frac{k}{n} = H(A)$. An arbitrarily low error probability can be achieved if

$$R = H(A) + \gamma < R_{\text{HDD}}. \quad (14)$$

The crossing point between the curves $H(A) + \gamma$ and R_{HDD} determines the optimal operating point [29], which could be achieved by a capacity-achieving code with infinitely large block length. In Fig. 4, we depict R_{HDD} and $R = H(A) + \gamma$ for different values of γ corresponding to some of the designed codes summarized in Table I. The corresponding code rate for a given γ , i.e., $(\frac{m-1+\gamma}{m})$ is also shown in Fig. 4. As can be seen, for $\gamma = 0.5233$ the curve $H(A) + \gamma$ is below R_{HDD} for all SNRs in the displayed SNR range. This means that with a single code of rate 0.8808, all the points on this curve are achievable by just changing the distribution of amplitudes in the PAS framework. However, for $\gamma = 0.6912$ and $\gamma = 0.7503$ only the points on the curve $H(A) + \gamma$ corresponding to SNRs larger than 22.36 dB and 23.66 dB, respectively, are achievable. Note that below these values, (14) is not satisfied. We highlight that, in principle, the points on the curve $H(A) + \gamma$ in the feasible SNR region are only achievable using codes with infinite code length. In practice, codes operate at finite length. For finite code length and a given γ , one can simulate the performance of the designed system and find the minimum SNR in the feasible SNR region required to achieve the desired block error probability.

B. Parameters of the PC

For a given ASK constellation and a given spectral efficiency, i.e., fixed γ and hence fixed PC rate R_{PC} , one can find several component BCH codes (v, t, s) that satisfy (8) and conditions (11), (12), and $n \in \mathbb{N}$, i.e., one can find several PCs that yield the desired spectral efficiency. Among them, we may then choose the one that yields the best decoding threshold, i.e., the lowest SNR at which the probability of error goes to zero for infinite block length. This approach leads, for each spectral efficiency, to the best possible PC and

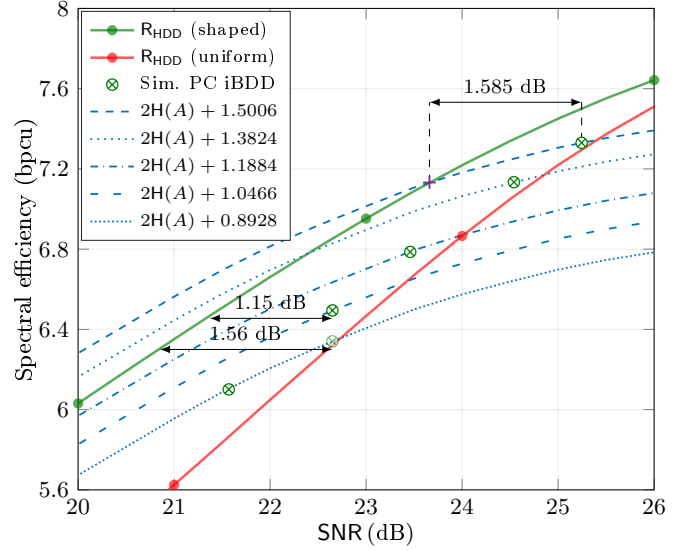


Fig. 5. Simulation results of the CM scheme for 256-QAM using the PCs summarized in Table I, and comparison with the corresponding achievable information rates.

therefore to the best performance. However, changing code for each spectral efficiency imposes extra complexity on the system, as different decoders should be implemented in the receiver which may not be desirable in practice. An alternative approach is to fix the parameters (v, t) of the component BCH codes and then tune the shortening parameter s , which leads to different γ and thus to different spectral efficiencies. With this approach one can cover a wide range of spectral efficiencies with only implementing a single PC decoder at the receiver digital signal processing block, which in turn reduces the decoder complexity significantly compared to the former approach. Similar approach has been taken for PAS and staircase codes as described in [35, Sec. V-B].

Note that since one can see square QAM constellations as the Cartesian product of two ASK constellations, the design of the PAS scheme described above readily extends to QAM constellations. In this case, the rate is twice that of the scheme with ASK constellation, i.e., $R = 2H(A) + 2\gamma$. In Fig. 2, the dashed block multiplexes two ASK modulated sequences corresponding to generate the real and imaginary components of the QAM constellation.

V. NUMERICAL RESULTS

We assess the performance of the CM scheme with PAS and HDD using the codes summarized in Table I for transmission using square QAM constellations. The target block error probability is set to $P_e = 10^{-3}$. Here, by block error probability we mean the probability that a block of bits of \mathbf{u}^a and \mathbf{u}^s corresponding to a PC code array is in error. By means of simulations, we find the minimum SNR for which the target P_e is achieved. At the receiver, the symbol-wise MAP detector in (4) is used and the decoding of the PC is performed using a maximum of 8 decoding iterations based on the BDD with extrinsic message passing [50, Algorithm 1].

To minimize the number of the operating modes, we consider the use of a single PC (according to the second approach

described in Section IV-B). In particular, we consider a PC with BCH component codes with parameters $(v, t) = (10, 3)$. To achieve different code rates, i.e., different spectral efficiencies, we then find suitable shortening parameters s which lead to a value of γ that satisfies (11), (12). Due to the space limitation, some of the feasible values of s and γ are summarized in Table I.

In Fig. 5, we plot the *practical operating points* of the PAS scheme for 256-QAM (green circle with crosses), corresponding to the minimum SNR required to achieve $P_e = 10^{-3}$. The optimal distribution $P_X^{\lambda^*}$ for an underlying 16-ASK constellation is used, where the 256-QAM is then obtained as the Cartesian product of two ASKs with distribution $P_X^{\lambda^*}$. The shortening parameters are 77, 261, 447, 535, and 605 (starting from the circle with crosses at the top right). The corresponding values of γ are given in the first row of Table I. Note that the simulation points are just a subset of size 5 out of 205 feasible practical operating points (see Sec. III-B). In fact we can vary the spectral efficiency with a very fine granularity to a larger and lower spectral efficiencies as that of shown in Fig. 5 by changing the shortening parameter and/or switching to a lower/higher order constellations. Remarkably, the rates achieved by the probabilistically-shaped CM scheme are larger than the achievable rate of the CM scheme with uniform signaling (red curve).

As an example, by finding the crossing point between the achievable rate curve and R_{HDD} for $\gamma = 0.7503$ ($s = 77$), marked with a red plus sign in Fig. 4, one can see that for all SNRs larger than 23.66 dB reliable transmission can be achieved. However, when using a practical, finite-length PC, one should back-off roughly 1.585 dB to meet the target P_e . We also remark that all points on the curves $2H(A) + 2\gamma$ with SNR larger than the minimum required SNR can also meet the target performance. However, since by increasing the SNR the curve $2H(A) + 2\gamma$ flattens out, at some point one needs to switch to another code rate (another γ) in order to operate as close as possible to the curve R_{HDD} . For instance, the faint circles with crosses on the achievable rate curve $2H(A) + 0.8928$ corresponding to $\gamma = 0.4464$ are also achievable, however, switching to $\gamma = 0.5233$ yields an operating closer the curve R_{HDD} , as shown in Fig. 4.

For the sake of comparison, we consider the same scenario using PAS and staircase codes decoded using sliding window with size 7 staircase blocks and 8 decoding iterations within the window, as considered in [35, Sec. VI]. In particular, to have fair comparison between staircase codes and PCs, we consider staircase codes with $(v, t) = (10, 3)$ and shortening parameters 63, 274, 431, 519, and 591, which gives virtually the same code rate as the PC code rates considered in Fig. 6. The performance of these codes is shown with green crosses. We remark that the performance of these codes was previously shown in [35, Fig. 8]. As can be seen for PCs, one need to back-off the SNR more than staircase codes, yielding higher spectral efficiencies at the cost of higher operating SNR. The lower operating SNR for staircase codes comes at the cost of higher decoding complexity and latency, as a window decoder is required. Furthermore, in Fig. 6, we compare the performance of PAS with PC and staircase code with the

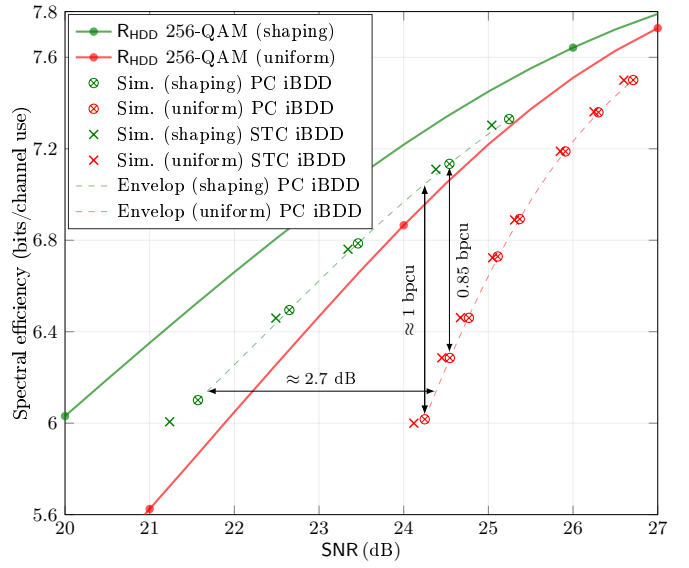


Fig. 6. Simulation results of the CM scheme for 256-QAM using PC and the staircase codes with parameters summarized in Table I and [35, Table. II]. comparison with the corresponding achievable information rates.

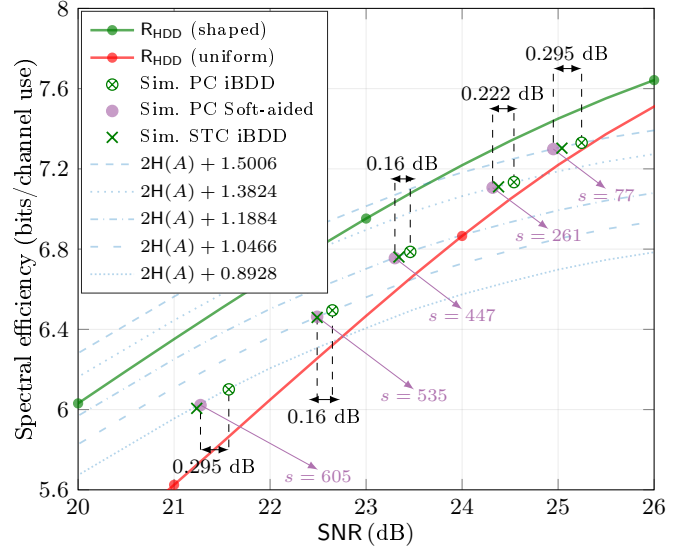


Fig. 7. Performance of the PAS with PC with soft-aided decoding algorithm, PC with iBDD, and staircase code with iBDD. Starting from top right, the shortening parameter for PC is 77, 266, 447, 535, and 605, and shortening parameter for staircase code is 63, 247, 431, 519, and 591.

corresponding system with uniform signaling. In particular, we consider PC with shortening parameters 77, 289, 447, 605, 661, 727, 759, and 797. These PCs have roughly the same code rate as staircase codes with shortening parameters 63, 271, 431, 591, 647, 711, 743, and 783 that are considered in [35, Fig. 8]. As can be seen the performance of the PAS with PC and PC with uniform signaling varies on an envelop (see green and red dashed curves in Fig. 6), where the performance improvement of PC with shaping over the uniform signaling reaches up to 2.7 dB. Furthermore, comparing the spectral efficiencies of PAS and PC with PC and uniformly distributed constellation points for a given operating SNR, one can see up to 1 bpcu improvement, e.g., PAS and PC with shortening parameter 261 has operating SNR 24.54 dB with spectral efficiency of 7.13 bpcu, while PC and uniformly distributed

constellation points with shortening parameter 743 and similar operating SNR provides the spectral efficiency of 6.28, i.e., 0.85 bpcu improvement as shown in Fig. 6. Comparing the simulation points with the corresponding AIR curve, it is clear that by reducing the code rate for both the PC and staircase codes, the SNR gap between practical operating points and the AIR increases, as expected since product-like codes with hard decision decoding are capacity achieving only for the asymptotically high rates [51]. We remark that for a given spectral efficiency this gap is always lower for the PAS with PC compared to PC with uniformly distributed constellation points. We remark that the same behavior can be seen for PAS with staircase codes as well.

Finally, in Fig. 7 we compare the performance of PAS with PC decoded using a variant of soft-aided decoding algorithm proposed in [12] with PAS and both PC and staircase code with iBDD. As shown in Fig. 7, PC with soft-aided decoding algorithm satisfy the target error probability in a lower SNR than PC with iBDD. Interestingly, PC with soft-aided decoding algorithm and shortening parameters 77, 261, and 447 provides a better operating point than that of staircase codes with iBDD and the same code rate (shortening parameters 63, 247, and 431), i.e., the required SNR for the same spectral efficiency is smaller. Furthermore, PC with soft-aided decoding algorithm and shortening parameter 519 provides the same performance as the corresponding staircase code code (shortening parameters 519) with iBDD, while the same architecture with shortening 605 provides slightly worse performance compared to the corresponding staircase code code (shortening parameters 591) with iBDD. We highlight that in this paper we used a pragmatic approach to find the operating points of the PAS with PC and soft-aided decoding algorithm, as the operating point of such architecture is still on the $2H(A) + 2\gamma$ curve, where $H(A)$ yielded form maximizing R_{HDD} (see (2)-(3)). In general, R_{HDD} is the achievable information rate of decoding system operating solely based on Hamming distance metric, while soft-aided decoder operates beyond Hamming metric as the channel reliabilities are employed in the decoding process. Therefore, the operating point shown in this paper can be improved further by finding the probabilistic shaping that maximizes the achievable information rate of the soft-aided decoding algorithm. An interesting line of research is to find the achievable information rate of the soft-aided decoding algorithms such as the ones proposed in [11]–[18]. This analysis is left as our further work.

VI. CONCLUSION

We applied probabilistic amplitude shaping to binary PCs with hard decision decoding for high-speed fiber-optic communications. We optimize the input distribution to maximize a relevant achievable rate of the CM system with PAS and bit-wise HDD. Outstandingly, the performance of the CM scheme with PAS is up to 2.7 dB better than that of the standard CM scheme with uniform distribution. We show that combining the soft-aided decoding algorithm with PAS for PC, and the performance of the system can be further improved up to 0.295 dB. As a result, interestingly, we show that PAS with PC and soft-aided decoding algorithm can outperform PAS with staircase codes and conventional iBDD.

REFERENCES

- [1] Fujitsu, “1FINITY T600 Transport Blade,” Online: <https://www.fujitsu.com/us/Images/1FINITY-T600-Data-Sheet.pdf>.
- [2] G. D. Forney and L. F. Wei, “Multidimensional constellations. I. Introduction, figures of merit, and generalized cross constellations,” *IEEE J. Sel. Areas Commun.*, vol. 7, no. 6, pp. 877–892, Aug. 1989.
- [3] B. S. G. Pillai, B. Sedighi, K. Guan, N. P. Ananthapadmanabhan, W. Shieh, K. J. Hinton, and R. S. Tucker, “End-to-end energy modeling and analysis of long-haul coherent transmission systems,” *IEEE/OSA J. Lightw. Technol.*, vol. 32, no. 18, pp. 3093–3111, Sep. 2014.
- [4] T. J. Richardson, M. A. Shokrollahi, and R. L. Urbanke, “Design of capacity-approaching irregular low-density parity-check codes,” *IEEE Trans. Inf. Theory*, vol. 47, no. 2, pp. 619–637, Feb. 2001.
- [5] R. M. Pyndiah, “Near-optimum decoding of product codes: block turbo codes,” *IEEE Trans. Commun.*, vol. 46, no. 8, pp. 1003–1010, Aug. 1998.
- [6] B. P. Smith, A. Farhood, A. Hunt, F. R. Kschischang, and J. Lodge, “Staircase codes: FEC for 100 Gb/s OTN,” *IEEE/OSA J. Lightw. Technol.*, vol. 30, no. 1, pp. 110–117, Jan. 2012.
- [7] C. Fougstedt and P. Larsson-Edefors, “Energy-efficient high-throughput VLSI architectures for product-like codes,” *IEEE/OSA J. Lightw. Technol.*, vol. 37, no. 2, pp. 477–485, Jan. 2019.
- [8] P. Elias, “Error-free coding,” *Trans. IRE Professional Group on Inf. Theory*, vol. 4, no. 4, pp. 29–37, Sep. 1954.
- [9] “Forward error correction for high bit-rate DWDM submarine systems,” ITU-T Recommendation G.975.1, 2004.
- [10] O. I. Forum, “Implementation agreement 400zr,” 2018.
- [11] A. Sheikh, A. Graell i Amat, and G. Liva, “Iterative bounded distance decoding of product codes with scaled reliability,” in *Proc. European Conf. Optical Communications (ECOC)*, Rome, Italy, 2018.
- [12] —, “Binary message passing decoding of product-like codes,” 2019. [Online]. Available: <https://arxiv.org/abs/1902.03575>
- [13] A. Sheikh, A. Graell i Amat, G. Liva, C. Häger, and H. D. Pfister, “On low-complexity decoding of product codes for high-throughput fiber-optic systems,” in *Int. Symp. on Turbo Codes & Iterative Inf. Proc. (ISTC)*, Hong Kong, Dec. 2018.
- [14] A. Sheikh, A. Graell i Amat, and G. Liva, “Binary message passing decoding of product codes based on generalized minimum distance decoding,” in *Proc. 53rd Annu. Conf. Inf. Sciences and Systems (CISS)*, Baltimore, MD, Mar. 2019.
- [15] C. Fougstedt, A. Sheikh, A. Graell i Amat, G. Liva, and P. Larsson-Edefors, “Energy-efficient soft-assisted product decoders,” in *Proc. Optical Fiber Commun. Conf. (OFC)*, San Diego, CA, USA, Mar. 2019.
- [16] C. Häger and H. D. Pfister, “Mis-correction-free decoding of staircase codes,” in *Proc. European Conf. Optical Communications (ECOC)*, Gothenburg, Sweden, Sep. 2017, pp. 1–3.
- [17] Y. Lei, A. Alvarado, B. Chen, X. Deng, Z. Cao, J. Li, and K. Xu, “Decoding staircase codes with marked bits,” in *Proc. Int. Symp. Turbo Codes and Iterative Inf. Processing (ISTC)*, Hong Kong, Dec. 2018, pp. 1–5.
- [18] G. Liga, A. Sheikh, and A. Alvarado, “A novel soft-aided bit-marking decoder for product codes,” 2019. [Online]. Available: <https://arxiv.org/abs/1906.09792>
- [19] J. Bellorado, M. Marrow, Z. Wu, and N. Kumar, “Decoding of turbo product codes using miscorrection detection,” 2018, US Patent US9565186 (B1).
- [20] V. D. Nguyen, K. S. Chilappagari, Z. Wu, and N. Kumar, “Systems and methods for hybrid message passing and bit flipping decoding of LDPC codes,” 2017, US Patent US9614548 (B1).
- [21] R. D. Cideciyan, R. A. Hutchins, T. Mittelholzer, and K. Tanaka, “Combination error and erasure decoding for product codes,” 2017, US Patent US2016006460 (A1).
- [22] M. F. Barsoum, C. Jones, and M. Fitz, “Constellation design via capacity maximization,” in *Proc. IEEE Int. Symp. Inf. Theory (ISIT)*, Nice, 2007, pp. 1821–1825.
- [23] T. Liu and I. B. Djordjevic, “Multidimensional optimal signal constellation sets and symbol mappings for block-interleaved coded-modulation enabling ultrahigh-speed optical transport,” *IEEE Photon. J.*, vol. 6, no. 4, pp. 1–14, Aug. 2014.
- [24] O. Geller, R. Dar, M. Feder, and M. Shtatif, “A shaping algorithm for mitigating inter-channel nonlinear phase-noise in nonlinear fiber systems,” *IEEE/OSA J. Lightw. Technol.*, vol. 34, no. 16, pp. 3884–3889, Aug. 2016.

- [25] B. Chen, C. Okonkwo, H. Hafermann, and A. Alvarado, "Increasing achievable information rates via geometric shaping," in *Proc. European Conf. Optical Communications (ECOC)*, Sep. 2018, pp. 1–3.
- [26] —, "Polarization-ring-switching for nonlinearity-tolerant geometrically shaped four-dimensional formats maximizing generalized mutual information," *IEEE/OSA J. Lightw. Technol.*, vol. 37, no. 14, pp. 3579–3591, Jul. 2019.
- [27] A. R. Calderbank and L. H. Ozarow, "Nonequiprobable signaling on the Gaussian channel," *IEEE Trans. Inf. Theory*, vol. 36, no. 4, pp. 726–740, Jul. 1990.
- [28] G. D. Forney, "Trellis shaping," *IEEE Trans. Inf. Theory*, vol. 38, no. 2, pp. 281–300, Mar. 1992.
- [29] G. Böcherer, F. Steiner, and P. Schulte, "Bandwidth efficient and rate-matched low-density parity-check coded modulation," *IEEE Trans. Commun.*, vol. 63, no. 12, pp. 4651–4665, Dec. 2015.
- [30] F. Buchali, F. Steiner, G. Böcherer, L. Schmalen, P. Schulte, and W. Idler, "Rate adaptation and reach increase by probabilistically shaped 64-QAM: An experimental demonstration," *IEEE/OSA J. Lightw. Technol.*, vol. 34, no. 7, pp. 1599–1609, Apr. 2016.
- [31] A. Ghazisaeidi, I. Fernandez de Jauregui Ruiz, R. Rios-Müller, L. Schmalen, P. Tran, P. Brindel, A. C. Mesequer, Q. Hu, F. Buchali, G. Charlet, and J. Renaudier, "Advanced C+L-band transoceanic transmission systems based on probabilistically shaped PDM-64QAM," *IEEE/OSA J. Lightw. Technol.*, vol. 35, no. 7, pp. 1291–1299, Apr. 2017.
- [32] C. Pan and F. R. Kschischang, "Probabilistic 16-QAM shaping in WDM systems," *IEEE/OSA J. Lightw. Technol.*, vol. 34, no. 18, pp. 4285–4292, Sep. 2016.
- [33] G. Böcherer, P. Schulte, and F. Steiner, "Probabilistic shaping and forward error correction for fiber-optic communication systems," *IEEE/OSA J. Lightw. Technol.*, vol. 37, no. 2, pp. 230–244, Jan. 2019.
- [34] J. Cho and P. J. Winzer, "Probabilistic constellation shaping for optical fiber communications," *IEEE/OSA J. Lightw. Technol.*, vol. 37, no. 6, pp. 1590–1607, Mar. 2019.
- [35] A. Sheikh, A. Graell i Amat, G. Liva, and F. Steiner, "Probabilistic amplitude shaping with hard decision decoding and staircase codes," *IEEE/OSA J. Lightw. Technol.*, vol. 36, no. 9, pp. 1689–1697, May 2018.
- [36] P. Poggiolini, "The GN model of non-linear propagation in uncompensated coherent optical systems," *J. Lightw. Technol.*, vol. 30, no. 24, pp. 3857–3879, Dec. 2012.
- [37] G. Böcherer, "Achievable rates for probabilistic shaping." [Online]. Available: <http://arxiv.org/abs/arXiv:1707.01134>.
- [38] G. Kaplan and S. Shamai, "Information rates and error exponents of compound channels with application to antipodal signaling in a fading environment," *AEU. Archiv für Elektronik und Übertragungstechnik*, 1993.
- [39] A. Lapidoth, "Mismatched decoding and the multiple-access channel," *IEEE Trans. Inf. Theory*, vol. 42, no. 5, pp. 1439–1452, Sep. 1996.
- [40] F. Gray, "Pulse code communication," US Patent 2632058, 1953.
- [41] F. R. Kschischang and S. Pasupathy, "Optimal nonuniform signaling for Gaussian channels," *IEEE Trans. Inf. Theory*, vol. 39, no. 3, pp. 913–929, May 1993.
- [42] G. Böcherer and R. Mathar, "Matching dyadic distributions to channels," in *Proc. Data Compression Conf. (DCC)*, Snowbird, UT, Mar. 2011, pp. 23–32.
- [43] S. Baur and G. Böcherer, "Arithmetic distribution matching," in *Proc. Int. ITG Conf. Systems, Communications and Coding (SCC)*, Hamburg, 2015, pp. 1–6.
- [44] R. A. Amjad and G. Böcherer, "Fixed-to-variable length distribution matching," in *Proc. IEEE Int. Symp. Inf. Theory (ISIT)*, Istanbul, 2013, pp. 1511–1515.
- [45] P. Schulte and G. Böcherer, "Constant composition distribution matching," *IEEE Trans. Inf. Theory*, vol. 62, no. 1, pp. 430–434, Jan. 2016.
- [46] T. Fehenberger, D. S. Millar, T. Koike-Akino, K. Kojima, and K. Parsons, "Multiset-partition distribution matching," *IEEE Trans. Commun.*, vol. 67, no. 3, pp. 1885–1893, Mar. 2019.
- [47] Y. C. Gültekin, W. J. v. Houtum, A. Koppelaar, and F. M. Willems, "Enumerative sphere shaping for wireless communications with short packets," 2019. [Online]. Available: <https://arxiv.org/abs/1903.10244>
- [48] C. Häger and H. D. Pfister, "Approaching miscorrection-free performance of product codes with anchor decoding," *IEEE Trans. Commun.*, vol. 66, no. 7, pp. 2797–2808, Jul. 2018.
- [49] J. Justesen, "Performance of Product Codes and Related Structures with Iterated Decoding," *IEEE Trans. Commun.*, vol. 59, no. 2, pp. 407–415, Feb. 2011.
- [50] Y. Y. Jian, H. D. Pfister, K. R. Narayanan, R. Rao, and R. Mazahreh, "Iterative hard-decision decoding of braided BCH codes for high-speed optical communication," in *Proc. IEEE Global Telecommun. Conf. (GLOBECOM)*, Atlanta, GA, 2013, pp. 2376–2381.
- [51] Y. Jian, H. D. Pfister, and K. R. Narayanan, "Approaching capacity at high rates with iterative hard-decision decoding," *IEEE Trans. Inf. Theory*, vol. 63, no. 9, pp. 5752–5773, Sep. 2017.